\$ SUPER

Contents lists available at ScienceDirect

## **European Polymer Journal**

journal homepage: www.elsevier.com/locate/europolj





# Star-shaped Poly(hydroxybutyrate)s from bio-based polyol cores via zinc catalyzed ring-opening polymerization of $\beta$ -Butyrolactone

Rawan Omar <sup>a</sup>, Muneer Shaik <sup>a</sup>, Chloe Griggs <sup>a</sup>, Jevin D. Jensen <sup>b</sup>, Robert Boyd <sup>b</sup>, Nuri Oncel <sup>b</sup>, Dean C. Webster <sup>c</sup>, Guodong Du <sup>a,\*</sup>

- <sup>a</sup> Department of Chemistry, University of North Dakota, 151 Cornell Street Stop 9024, Grand Forks, ND 58202, United States
- b Department of Physics and Astrophysics, University of North Dakota, 101 Cornell Street Stop 7129, Grand Forks, ND 58202, United States
- <sup>c</sup> Department of Coatings and Polymeric Materials, North Dakota State University, Fargo, ND 58108, United States

#### ARTICLE INFO

#### Keywords: Poly(β-hydroxybutyrates) Ring-opening polymerization Star polymers β-butyrolactone Zinc catalysis

#### ABSTRACT

The ring-opening polymerization (ROP) of cyclic esters using multifunctional initiators is an efficient methodology that allows the preparation of polyesters with well-defined architectures. Here a series of star-shaped poly ( $\beta$ -hydroxybutyrates) (PHBs) has been synthesized by ROP of  $\beta$ -butyrolactone (BBL) with an amido-oxazolinate zinc catalyst. The star-shaped structure is constructed via a core-first approach, in which several bio-based multifunctional alcohols serve as the initiator for ROP. Specifically, three-, four-, and multi-armed star polymers are obtained and characterized by various techniques including NMR, GPC, TGA, and DSC, and the incorporation of the core structure in the star-shaped PHBs has been confirmed. The thermal properties can be modified by changing the arm number and arm length of PHBs, and the thermal stability decreases as the number of arms increases when they have the same arm lengths. The wetting behavior determined from AFM studies demonstrates a minimum in the macroscopic contact angle as a function of the number of arms of a star-shaped

#### 1. Introduction

Aliphatic polyesters such as poly(hydroxyalkanoates) (PHAs) have recently received much attention as environmentally friendly materials, and have been widely used in a variety of applications ranging from packaging to medicine. [1.2] One of the subclasses, poly( $\beta$ -hydroxybutyrates) (PHBs), has emerged as alternative materials to petroleumbased plastics due to their biodegradability, biocompatibility, and enhanced thermal and mechanical properties.[3] PHBs produced naturally by microorganisms have a highly isotactic and crystalline structure that leads to a high melting temperature  $(T_m)$ . [4,5] The most convenient synthetic method for PHBs is the ring-opening polymerization (ROP) of  $\beta$ -butyrolactone (BBL) with a catalyst, which has the advantage of producing polymers with well-controlled molecular weight  $(M_n)$  and narrow dispersity (D).[6-9] As an abundant and biocompatible metal, Znbased catalysts bearing various ancillary ligands have displayed high activity for the synthesis of a number of different biodegradable polyesters in general[10-17] and PHBs from ROP of BBL in particular. [18-21]

In recent years, increasing efforts have been directed to polymers with unique structures and topological properties that are otherwise inaccessible in the case of linear polymers. Because of their peculiar morphologies and the higher functional group concentrations, the starshaped polymers may have different properties such as smaller hydrodynamic radii, lower viscosities, and suitable thermal properties for biomedical and drug delivery applications. [22-26] Hillmyer and coworkers recently reported a series of multi-arm star poly(lactide)s (PLA) that was better than the linear analogue in preparing expanded PLA foams with low densities.[27] The synthetic routes for star-shaped polymers can be generally classified into the "core-first", "arm-first", and "grafting-onto" approaches.[28] Among them, the "core-first" approach has been extensively used for producing well-defined multiarmed polymeric architectures with a range of predefined numbers in the multi-functional initiators.[29-31] The use of multifunctional alcohols as initiators and/or chain transfer agents offers advanced architectures with properties inherited from the functional moieties.[32] Despite the intensive interest in these architectures, detailed studies of star-shaped PHBs generated through ROP of BBL are rare.[33,34]

E-mail address: guodong.du@und.edu (G. Du).

 $<sup>^{\</sup>ast}$  Corresponding author.

Scheme 1. Synthesis of star-shaped PHBs with various initiator core structures.

Previously, we have shown that amido-oxazolinate zinc complexes are efficient catalysts for the controlled ROP of BBL in the presence of mono- and bifunctional alcohols, resulting in the formation of linear PHBs with well-defined end groups, whereas high molecular weight cyclic PHBs are produced in the absence of an alcohol. [35] Built on these results, herein we report a series of star-shaped PHBs with different initiator core structures (Scheme 1). Glycerol (GLY) and pentaerythritol (PE) were used to form three- and four-armed stars, and high functionality polyols such as methoxylated sucrose soyate polyol (MSSP) and hydroxylated sucrose soyate (HSS) were employed to produce multiarmed stars. All these core initiators are and/or can be derived from biorenewable resources. Glycerol is a major byproduct in biodiesel industry, [36] and PE has been prepared by condensation of bio-sourced acetaldehyde[37] with formaldehyde. Sucrose esters of unsaturated fatty acids, the precursor for MSSP and HSS, were developed by combining carbohydrates and plant oils[38] and have been utilized as thermosetting materials and drug delivery platform.[39,40] The obtained polymers were thoroughly characterized and investigated for their thermal and wetting properties by various techniques. The effect of the number and the length of the arms were studied and compared with the linear PHBs since it was expected that branched architectures might have different features.

## 2. Experimental section

#### 2.1. Materials and methods

All reactions involving air- and/or moisture-sensitive compounds were performed under a dry nitrogen atmosphere using standard Schlenk line and glovebox techniques. CDCl $_3$  was purchased from Cambridge Isotope Laboratories and distilled over CaH $_2$  and degassed prior to use. THF (HPLC grade, Fisher Scientific), dichloromethane, hexane and acetone (Sigma-Aldrich) were purchased commercially and used as received. Toluene was distilled under nitrogen from Na/benzophenone.  $\beta$ -Butyrolactone (BBL) was distilled over CaH $_2$  following three freeze–pump–thaw cycles. Glycerol was dried over activated

molecular sieves (4 Å) prior to use. Pentaerythritol was dried under vacuum overnight. Methoxylated sucrose soyate polyol (MSSP) and hydroxylated sucrose soyate (HSS)[41] were obtained according to the literature and determined to have  $\sim 12$  and  $\sim 24$  hydroxyl groups, respectively (see Scheme 1 for their structures). They were diluted in dry toluene and stored with pre-activated 4 Å molecular sieves. The zinc catalyst  $\bf Zn-1$  was synthesized according to the literature. [42,43]

NMR spectra (1D and 2D) were recorded on a Bruker AVANCE 500 NMR spectrometer and referenced to the residual peaks of CDCl $_3$ . Gel permeation chromatography (GPC) analysis was performed on a Varian Prostar instrument equipped with a PLgel 5  $\mu$ m Mixed-D column, a Prostar 355 RI detector, and THF as eluent at a flow rate of 1 mL/min (20 °C). Polystyrene standards were used for calibration. Thermal gravimetric analysis (TGA) was performed on an SDT Q 600 instrument at a flow rate of 100 mL/min of N $_2$  (furnace purge gas). The samples in aluminum oxide (Al $_2$ O $_3$ ) cups were heated from 30 to 600 °C with a ramp rate of 20 °C/min. Advantage software was used to analyze the TGA data. Differential scanning calorimetry (DSC) was performed on a PerkinElmer Jade differential scanning calorimeter with a 20.0 °C/min heating rate from -20 °C to 160 °C under 20 mL/min nitrogen flow. The instrument was calibrated using zinc and indium standards. DSC data was analyzed using Pyris V9.0.2 software.

### 2.2. General procedure for star-shaped PHBs

All catalytic reactions were performed under an inert atmosphere, and a representative procedure with glycerol is described here in detail. In a glovebox under dry nitrogen, an oven-dried 10 mL Schlenk flask with a stir bar was charged with zinc catalyst (3 equiv, based on the arm number), glycerol initiator (1 equiv), BBL (300 equiv, [100 equiv  $\times$  arm number]), and toluene (so that the total volume was 4.0 mL). The flask was capped and taken out, and then heated in an oil bath at 100 °C until the complete conversion of BBL was observed by  $^1$ H NMR spectroscopy. After removal of the volatile components under vacuum, the resulting residue was dissolved in DCM (1–3 mL), followed by addition of hexane (4–5 mL). The precipitation of the polymeric product was facilitated by

Table 1 ROP of rac-β-butyrolactone using catalyst **Zn-1** with glycerol. <sup>a</sup>

Entry	Zn/Gly/BBL	[BBL]/M	Time	$M_{\rm n}({ m Calcd})^b$	$M_{\rm n}({\rm NMR})^c$	$M_{\mathbf{n}}(\mathbf{GPC})^d$	$\mathbf{\tilde{D}}^{\mathbf{d}}$	Yield %
1	3:1:30	0.14	60 min	2.7	2.7	n.d.	n.d.	78
2	3:1:300	1.40	60 min	25.9	25.3	6.7	1.31	82
3	3:1:600	2.81	80 min	51.7	60.4	16.6	1.38	86
4	3:1:1200	5.62	90 min	103.4	104.5	27.8	2.02	90
5	3:10:600	2.81	80 min	5.3	6.5	6.1	1.29	88
6	3:20:600	2.81	90 min	2.7	2.9	n.d.	n.d.	84

<sup>&</sup>lt;sup>a</sup> Polymerizations were run in toluene at 100 °C, and monitored by NMR until all BBL was consumed (100% conversion). The molecular weights are reported in kg/mol and the yields refer to isolated yields of PHBs. n.d.: not determined. <sup>b</sup>Calculated on the basis of conversion and catalyst/initiator loading. <sup>c</sup>Determined by the end-group/main-chain ratio in <sup>1</sup>H NMR. <sup>d</sup>Determined by GPC calibrated with polystyrene standards in THF without correction.

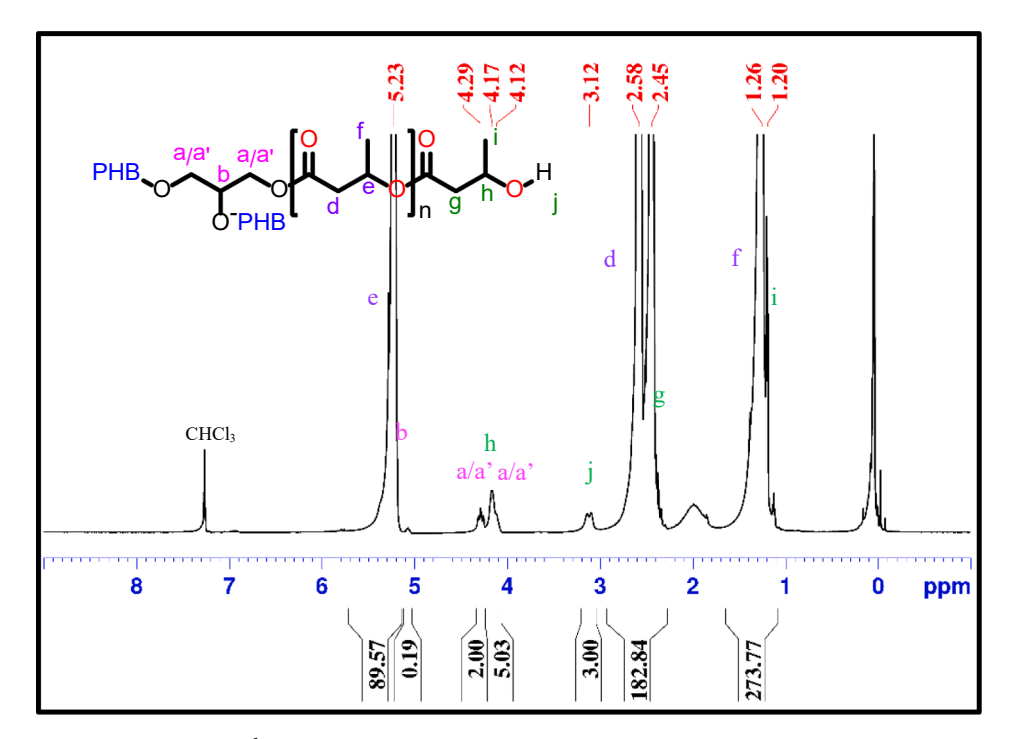


Fig. 1. <sup>1</sup>H NMR spectrum of the PHB with glycerol core (Table 1, entry 6).

cooling the flask briefly in liquid nitrogen, and the supernatant was decanted. After purification, the polymer was dried in a vacuum to constant weight to determine the yield and characterized by various techniques,

#### 2.3. AFM experiments

The atomic force microscopy (AFM) was performed on an ez-AFM instrument from Nanomagnetics Inc. A series of star-shaped PHBs with arm length of  $\sim 100$  repeating monomer units were selected for AFM studies. Dilute solutions of polymers were prepared in acetone. The solutions were spin-coated on freshly cleaved mica surfaces. All the AFM images were measured in tapping mode at room temperature under ambient conditions. Gwiyddion software was used to process and analyze all AFM images.  $\cite{[44]}$ 

#### 3. Results and discussion

## 3.1. ROP of BBL with glycerol

A three-armed star-shaped PHB having hydroxyl end groups was first synthesized by ROP of BBL initiated from glycerol as the tri-functional initiator in toluene at 100  $^{\circ}\text{C}$  with catalyst **Zn-1**, following the standard conditions employed in the previous study.[35] The corresponding results at different ratios of Zn/Gly/BBL are summarized in Table 1. As

shown in Table 1, 100 % of monomer conversion was achieved within 60–90 min when the reaction was performed at different ratios of Zn/Gly/BBL. Number average molecular weights ( $M_n$ ) up to 103.4 kg/mol were obtained, and good agreements between experimental (by NMR) and calculated values were observed (Table 1, entries 1–4). On the other hand, the lower molecular weight observed by GPC (without applying a correction factor) can be attributed to the smaller hydrodynamic volume of star-shaped and branched macromolecules compared to the linear polystyrene standards.[45–47] Up to 20 equivalents of hydroxyl initiating groups from glycerol (Table 1, entries 5–6) could be applied, leading to formation of low molecular weight products, which indicated that glycerol could act as effective chain transfer agent.

The microstructure of the PHBs with glycerol was studied by NMR spectroscopic techniques. Fig. 1 shows a representative  $^1H$  NMR spectrum of the PHB obtained with a ratio of [Zn]/[Gly]/[BBL] = 3:20:600 (entry 6 in Table 1). The strong signals at 5.23, 2.59–2.47, and 1.26 ppm could be assigned to the methine (e), methylene (d), and methyl (f) protons, respectively, of the main chain butyrate units. A small peak h at 4.17 ppm was attributed to the methine protons of the terminal butyrate units, and the corresponding methylene and methyl protons (peak g and i) overlapped with the large main chain signals (peaks d and f). The chain end hydroxyl group could be observed at 3.12 ppm. Importantly, the small peaks at 4.12 ppm and 4.29 ppm could be assigned to the diastereotopic methylene protons (a/a') of the glycerol unit, while the glycerol methine proton (b) was buried under the main chain methine

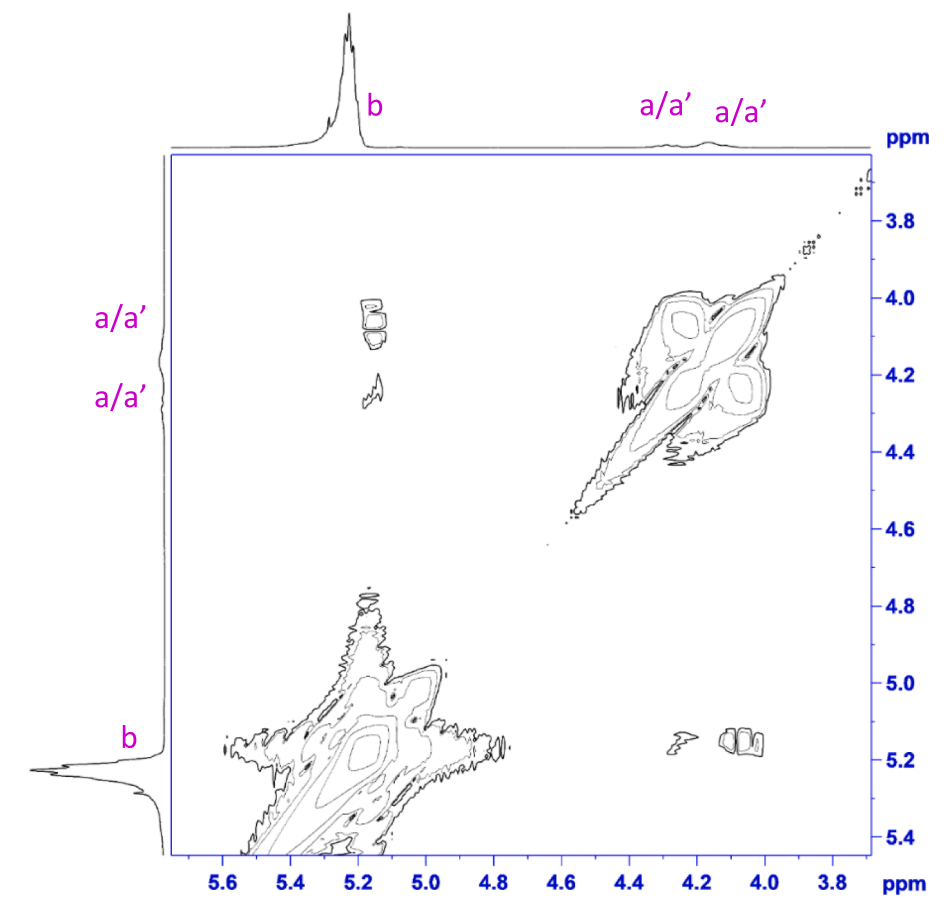


Fig. 2. Part of the <sup>1</sup>H-<sup>1</sup>H COSY NMR spectrum of the PHB with glycerol (Table 1, entry 6).

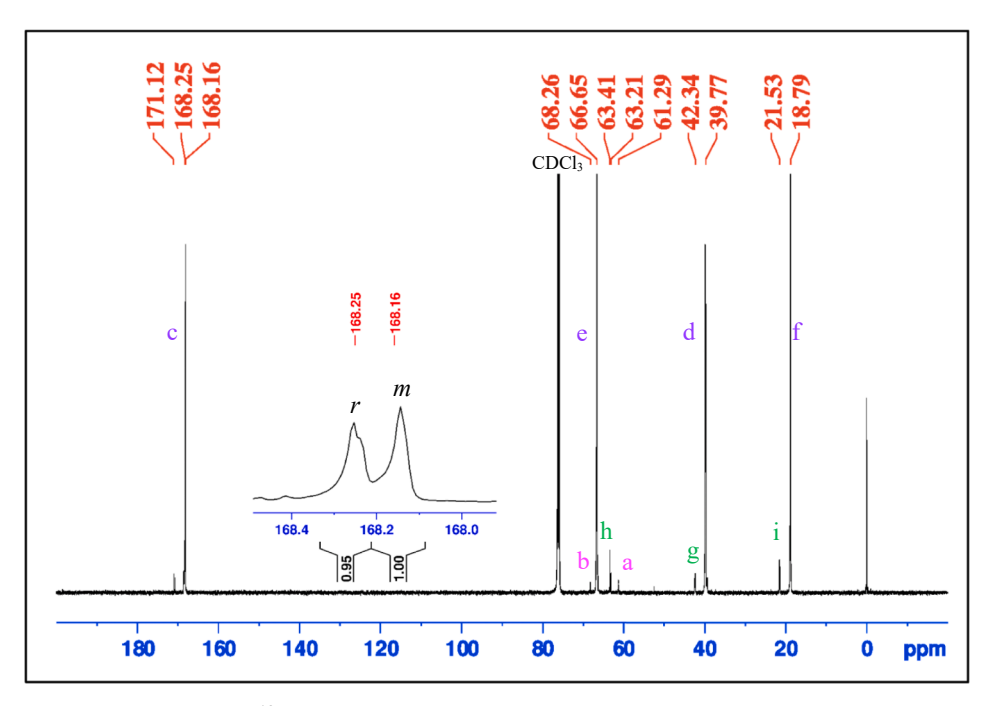


Fig. 3.  $^{13}$ C NMR spectrum of the PHB with glycerol (Table 1, entry 6).

signal at 5.23 ppm, but could be discerned by the off-diagonal signals in a 2D COSY experiment (Fig. 2). The DOSY NMR of a Gly 3–1-30 sample showed that the glycerol methylene signals around 4.2 ppm aligned with the main chain PHB components (Figure S14). These observations

supported that glycerol was incorporated into the polymer structure as the core and all three hydroxyl groups served as the initiators. Although both primary and secondary hydroxyl groups with different reactivity are present in glycerol, once the initial propagation at the primary OH

Table 2 ROP of rac-β-butyrolactone using catalyst **Zn-1** with pentaerythritol. <sup>a</sup>

Entry	Zn/PE/BBL	Time	$M_n(Calcd)^b$	$M_{\rm n}({\rm NMR})^c$	$M_{\rm n}({ m GPC})^d$	$\mathbf{D}^d$	Yield %
1	4:1:40	1 h	3.6	3.4	1.4	1.20	68
2	4:1:100	1 h	8.7	9.5	2.4	1.32	75
3	4:1:400	1 h	34.6	42.6	14.3	3.07	84
4	4:1:800	1.5 h	69.0	69.1	21.4	2.10	88
5	4:10:800	4 h	7.0	17.4	15.9	1.15	86
6	4:50:800	3 h	1.5	1.0	n.d.	n.d.	67

<sup>&</sup>lt;sup>a</sup> Polymerizations were run in toluene at 100 °C and monitored by NMR until all BBL was consumed (100% conversion). The molecular weights are reported in kg/mol and the yields refer to isolated yields of PHBs. n.d.: not determined. <sup>b</sup>Calculated on the basis of conversion and catalyst/initiator loading. <sup>c</sup>Determined by the end-group/main-chain ratio in <sup>1</sup>H NMR. <sup>d</sup>Determined by GPC calibrated with polystyrene standards in THF.

takes place, the propagating ends become secondary, so all three hydroxyl groups would have comparable activity for enchainment. The structural assignment was also supported by <sup>13</sup>C NMR spectroscopy (Fig. 3). Besides the carbon signals attributed to the main chain and the chain end resonances of the butyrate units, [35] the peaks a/a' and b at 61.29 and 68.26 ppm could be assigned to methylene and methine carbons of the glycerol moiety, respectively, which are supported by <sup>1</sup>H–<sup>13</sup>C HETCOR NMR spectrum (Figure S2). Furthermore, the two peaks of roughly equal intensity at the carbonyl region (inset, Fig. 3) suggest the PHB is atactic, consistent with earlier observations with such zinc catalysts.[35] The ESI-MS analysis (Figure S3) of a glycerolinitiated PHB (Table 1, Entry 1) showed a dominant series of peaks at 89 + 86n + 3H + 18 that could be assigned to  $C_3H_5O_3 + n(C_4H_6O_2) +$  $3H + NH_4^+$  structure, consistent with the NMR assignments. These observations indicated that all three hydroxyl groups of glycerol effectively initiated ROP of BBL as the star core with PHB arms.

#### 3.2. ROP of BBL with pentaerythritol

Four-armed star-shaped PHBs were prepared following a similar procedure. Thus, pentaerythritol (PE) was used as a tetra-functional initiator, whereas the hydroxyl end groups of the PE core initiated ROP of BBL, and the results are summarized in Table 2. In most cases complete conversions were achieved within 1 h, and the resulting PHBs were largely atactic, as determined by inverse gated <sup>13</sup>C NMR. As observed before, relatively narrow dispersities (£ 1.15-1.34) were obtained, and theoretical and experimental molecular weights by NMR exhibited a reasonable agreement, while the GPC (Figure S13) determined molecular weights were lower. Furthermore, higher loading of alcohol (up to 12 equivalents of PE vs catalyst) could be employed, and the molecular weights of the polymers decreased according to the initiator/Zn ratios, indicating that alcohols also acted as chain transfer agents in the reaction. This provided a way to control the molecular weights by changing the Zn/alcohol ratios. A conversion-time profile of the four-armed PHBs formation (Figure S9) suggested that the reaction approximately followed the first order kinetics, and the number of propagation chains remained constant throughout the reaction. [30]

The <sup>1</sup>H NMR analysis (Figure S4) of a representative sample ([Zn]/[PE]/[BBL] = 4:1:400) revealed the presence of methylene resonance at

4.09 ppm (peak a) corresponding to the PE moiety, and the chain end was characterized by a terminal hydroxybutyrate unit featuring a singlet at 4.17 ppm (peak h) for the methine protons and a doublet at 3.09 ppm for hydroxyl protons (peak j), which confirmed the presence of the PE unit as the central core. The ratio of the integrations of the 3.09 ppm peak (the butyrate hydroxyl, 4H) vs the 4.1 ppm peak (PE methylene, 8H; and the butyrate chain end methine CH, 4H) was approximately 4:12, in agreement with them being the four ends of the chain. The presence of the PE core was also supported by the <sup>13</sup>C NMR spectrum (Figure S5), where two signals at 62.3 ppm (CCH<sub>2</sub>) and 43.5 ppm (CCH<sub>2</sub>) were observed. Together, these observations supported that the PE unit was incorporated into the core and the polymer end groups were hydroxybutyrate. As in the cases of diol initiators, [35] the presence of a small amount of olefin end groups were sometimes observed as a result of the dehydration of hydroxyl groups.

## 3.3. ROP of BBL with high functionality polyols

In addition to the glycerol and PE cores, branched methoxylated sucrose soyate polyol (MSSP) and hydroxylated sucrose soyate (HSS), considered as highly functional bio-based polyols, were used as the macromolecular initiators for the ROP of BBL to obtain the star-shaped PHBs. Biobased polyols such as methyoxylated epoxidized sucrose soyate (MSSP) have been employed to give polyurethanes having higher modulus, hardness, and glass transition temperatures ( $T_{\rm g}$ ) compared to soy-based and petroleum-based polyols.[48–50] Herein, we show that these polyols can act as a central core to create well-fashioned star polyesters.

The polymerization of BBL was carried out with MSSP in the presence of catalyst **Zn-1** in toluene at 100 °C as shown earlier. The results of the polymerization using different amount of BBL monomer are presented in Table 3. BBL in most of the reactions was completely consumed within 60 min, and the isolated yields of the polymers were typically 60–90 % (Table 3, entries 1–4). In a similar manner, star-shaped PHBs were synthesized by ROP in the presence of catalyst **Zn-1** and HSS as the core initiator (Table 3, entries 5 and 6), and polymers with higher arm numbers and different chain lengths could be obtained in good yields. However, the resultant molecular weights in these cases were smaller than the molecular weights calculated from conversion and catalyst

Table 3
ROP of *rac-*β-butyrolactone using catalyst **Zn-1** with MSSP and HSS. <sup>a.</sup>

Entry	Zn/I/BBL	Time	$M_n(Calcd)^b$	$M_{\rm n}({\rm NMR})^c$	$M_{\rm n}({ m GPC})^d$	$\mathbf{D}^d$	Yield %
1	12:1:120	60 min	13.4	9.1	9.3	1.20	58
2	12:1:1200	60 min	106.3	35.4	38.4	1.78	74
3	12:1:2400	60 min	209.6	169.9	132.8	1.27	82
4	12:1:4800	90 min	416.3	38.5	25.0	1.25	89
$5^{e}$	24:1:240	60 min	23.6	8.8	n.d.	n.d.	67
6 <sup>e</sup>	24:1:2400	180 min	209.5	71.8	n.d.	n.d.	78

<sup>&</sup>lt;sup>a</sup> Polymerizations were run in toluene at 100 °C, and monitored by NMR until all BBL was consumed (100% conversion) except for entry 2, where 90% conversion was noted. The molecular weights are reported in kg/mol and the yields refer to isolated yields of PHBs. n.d.: not determined. <sup>b</sup>Calculated on the basis of conversion and catalyst/initiator loading. <sup>c</sup>Determined by the end group/main chain ratio in <sup>1</sup>H NMR. <sup>d</sup>Determined by gel permeation chromatography calibrated with polystyrene standards in THF. <sup>e</sup>HSS was used as the core.

**Table 4**Thermal properties of star-shaped PHBs. a, b.

Entry	Polymers	$T_{-5\%}$	$T_{-50\%}$	$T_{-95\%}$	$T_{max}$	$T_{g}$
Table 1, entry 2	Gly 3-1-300	256	310	388	311	5.3
Table 1, entry 3	Gly 3-1-600	277	297	300	302	8.0
Table 1, entry 4	Gly 3-1-1200	151	310	322	312	-2.6
Table 1, entry 5	Gly 3-10-600	256	296	317	302	4.9
Table 1, entry 6	Gly 3-20-600	255	310	386	310	-6.4
Table 2, entry 2	PE 4-1-100	N/A	N/A	N/A	N/A	5.6
Table 2, entry 3	PE 4-1-400	272	291	352	292	8.3
Table 2 entry 4	PE 4-1-800	279	294	296	300	7.6
Table 2, entry 5	PE 4-10-800	245	277	295	281	5.4
Table 3, entry 2	MSSP 12-1-1200	254	278	497	281	6.0
Table 3, entry 3	MSSP 12-1-2400	262	290	294	299	1.4
Table 3, entry 4	MSSP 12-1-4800	267	291	301	302	2.5
Table 3, entry 6	HSSP 24:1:2400	238	283	286	284	n.d.

 $^a\mathrm{Temperatures}$  in  $^{\circ}\mathrm{C}$ .  $^bT_\mathrm{g}$  were determined from the second heating cycle in DSC.  $T_{-5\%},\ T_{-5\%},\ T_{-5\%}$ , and  $T_{-95\%}$  refer to the temperatures at which 5%, 50%, and 95% weight losses were observed in TGA, respectively.  $T_\mathrm{max}$  refers to the temperatures at which the maximum rate of weight loss occurs.

loading. The dispersities ( $\theta=1.09-1.87$ ) were relatively broad, which can be attributed to the fact that there is a distribution of functionalities in MSSP and HSS.[47]

A representative <sup>1</sup>H NMR spectrum of the star-shaped PHBs obtained with MSSP as a central core is shown in Figure S7. Besides the main chain butyrate signals at 1.26, 2.45 and 2.59, and 5.25 ppm (peak f, d, and e, respectively) and the methine protons of the chain end at 4.18 ppm, there are additional signals that match the MSSP core structures. For instance, the peak at 3.38 ppm (peak n) can be assigned to the methoxy protons of the central core, whereas the methine protons (peak m') adjacent to the oxygen of the ester groups show signals at 4.26 ppm. Moreover, the triplet signal (peak a) at 0.87 ppm corresponds to the terminal methyl protons of the MSSP core. Similarly, the resonance peaks of the butyrate repeating units of PHBs and the HSS core were clearly observed in the <sup>1</sup>H NMR spectrum of the star polymers synthesized with HSS (Figure S8). These results provide evidence that MSSP and HSS had been incorporated with the hydroxybutyrate to form the star-shaped PHBs.

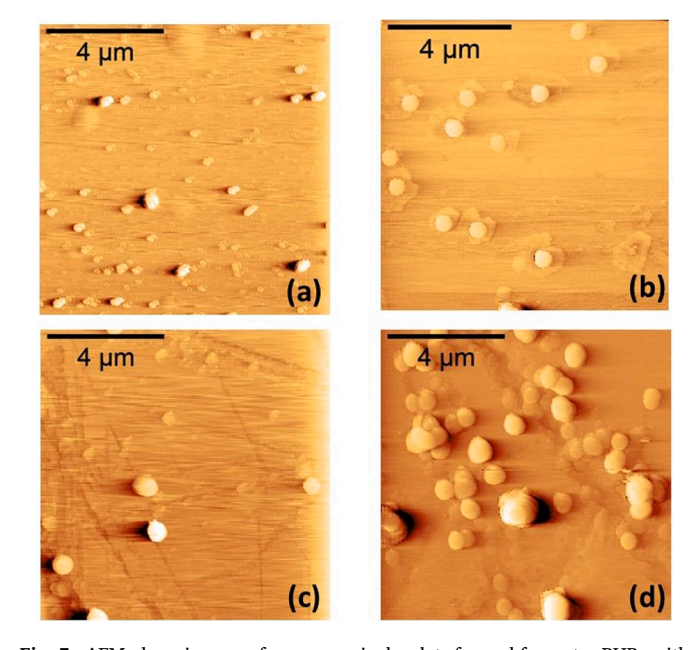
#### 3.4. Thermal properties

Commonly, star-shaped polymers with a higher arm number and arm length exhibit faster thermal decomposition and noticeably lower thermal transition when compared with their linear counterparts with the same monomer/initiator ratio. [46] With the use of the same monomer/initiator ratio, the glass transition temperature ( $T_g$ ) and the temperature of maximum decomposition ( $T_{max}$ ) of the star-shaped PHBs decreased as either the arm numbers increased, or the arm lengths decreased. [51,52] To study the effects of the arm number and arm length on thermal properties, the differential scanning calorimetry

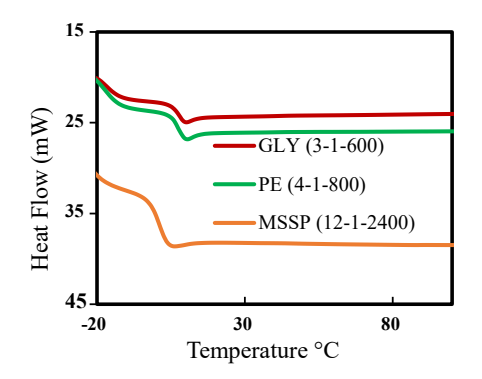
(DSC) and thermogravimetric analysis (TGA) methods were conducted on the prepared star-shaped PHBs, and the characteristic results are summarized in Table 4.

The  $T_{\rm g}$  values of star PHBs with glycerol and PE as the core were found to be comparable to that of linear PHBs. For instance, the  $T_{\rm g}$  of star-shaped PHB with glycerol as the core was 8.0 °C, comparable to the linear PHBs with similar length of repeating units. When the arm numbers increased with the use of MSSP as a core, the  $T_{\rm g}$  decreased to 1.4 °C. As shown in Fig. 4, the  $T_{\rm g}$  shifted to lower temperatures as the arm numbers increased. These results demonstrated that arm number of polymers can affect the  $T_{\rm g}$  values. Furthermore, the arm lengths could also play a role in determining the  $T_{\rm g}$  of PHBs. Herein, the  $T_{\rm g}$  of the star-shaped PHBs with the same arm numbers but different arm lengths, were investigated and exhibited lower  $T_{\rm g}$  value when the arm lengths decreased, as shown in Figures S10-S12. These observations provide support that the thermal properties of PHBs could be modified by changing the arm number and arm length of PHBs.

The thermal stability of the star-shaped PHBs was analyzed by TGA in the temperature range of 30–600 °C. Fig. 4 shows a comparison of the thermal decomposition temperature of the synthesized PHBs with different arm numbers. The TGA data (Table 4) and thermograms indicated that the onset ( $T_{.5\%}$ ) and the maximum decomposition ( $T_{max}$ ) of the star-shaped PHBs were lower than those of linear and cyclic PHBs. This reduced thermal stability may be related to the increase of



**Fig. 5.** AFM phase images of macroscopic droplets formed from star PHBs with GLY (a), PE, (b), MSSP (c), and HSS (d) cores.



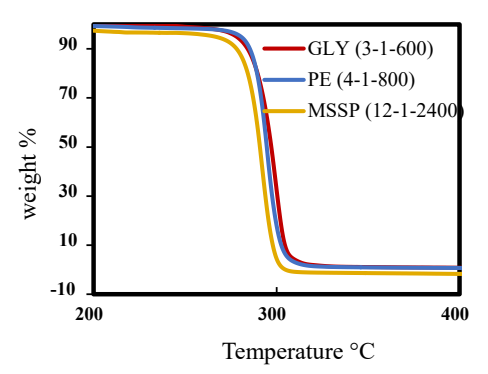


Fig. 4. DSC (left) and TGA (right) thermograms of star-shaped PHBs.

**Table 5**Average height, radius and contact angle of the polymer droplets on mica.

Polymer	Average Height (nm)	Average Radius (μm)	Average Contact Angle (degrees)
GLY 3-1-300 PE 4-1-400 MSSP 12-1- 1200 HSS 24-1- 2400	12.9 8.54 29.7 21.2	0.30 0.53 0.67 0.43	$4.56 \pm 1.75$ $1.81 \pm 0.52$ $1.97 \pm 0.61$ $4.20 \pm 1.83$

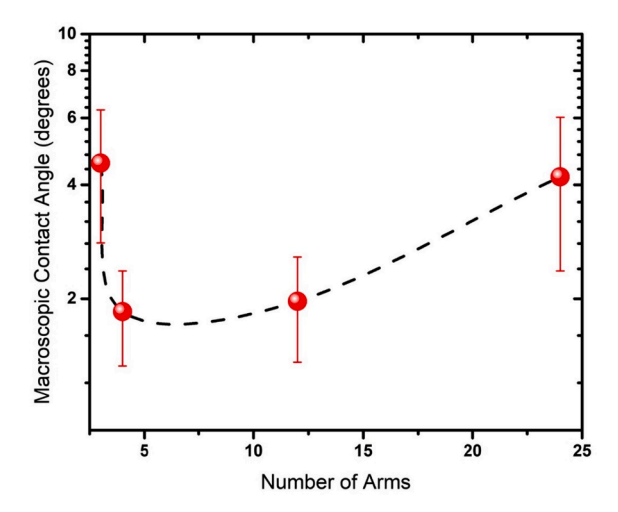


Fig. 6. The macroscopic contact angle vs. the number of arms.

thermally unstable hydroxyl end groups. [51]. The decomposition showed a single stage profile, and the MSSP-derived PHBs exhibited the lowest thermal decomposition temperature among the three. Comparatively, the thermal stability of the obtained PHBs decreased in the order PHB-glycerol > PHB-PE > PHB-MSSP, although they have the same arm lengths.

#### 3.5. AFM studies

The morphology of a series of star-shaped PHBs on hydrophilic mica surface was studied with AFM under ambient conditions. In the AFM images (Fig. 5), we observed the formation of macroscopic droplets, and the height (H), and radius ( $R_D$ ) of the droplets are summarized in Table 5. For GLY (3–1-300), in addition to macroscopic droplets, we observed a collection of smaller droplets with diameters of a couple of hundred nanometers. The formation of the smaller droplets indicates that its wetting process resembles that of linear polymers.[53]

The ability to control wetting is crucial for several technological applications such as protective coatings, lubricants, and sensors. Here we focus on the wettability of these star-shaped polymers to investigate the correlation between the number of arms (f) and the wettability. The macroscopic contact angles,  $\theta_{\infty}$ , of the macroscopic droplets were extracted using the relation  $\tan\left(\frac{\theta_{\infty}}{2}\right) = H/R_D$ , and plotted against the number of arms in the polymers (Fig. 6). As can be seen,  $\theta_{\infty}$  drops sharply first and then increases as the number of arms increases, similar to the observation with a series of star-shaped polystyrenes. [54] The wetting behavior of star-shaped molecules is determined by two competing factors. The wettability increases as the number of arms increases because, for large f, the decrease in entropy is less significant upon adsorption. On the other hand, an increasing number of arms causes opposing soft steric entropic repulsion which limits the probability of polymers being adsorbed and forming close-packed droplets onto surfaces. These competing effects lead to a minimum in the

macroscopic contact angle as a function of the number of arms of a star-shaped polymer.

#### 4. Conclusions

In summary, a series of biodegradable and well-defined star-shaped PHBs with different arm numbers and arm lengths were successfully synthesized using Zn catalyzed ROP of BBL in the presence of polyol initiators. The efficient initiation by the three, four-, and multi-armed cores was confirmed by the NMR analysis. The thermal properties such as  $T_{\rm g}$  and  $T_{\rm max}$  of the obtained star-shaped PHBs depended upon their arm numbers as well as their arm lengths, and the wetting behavior could be correlated to the arm numbers. Future research will focus on expanding this methodology to include the incorporation of other monomers.

#### CRediT authorship contribution statement

Rawan Omar: Investigation, Formal analysis, Writing – original draft. Muneer Shaik: Investigation, Formal analysis, Data curation, Writing – original draft. Chloe Griggs: Investigation, Formal analysis. Jevin D. Jensen: Investigation, Formal analysis. Robert Boyd: Investigation, Formal analysis. Nuri Oncel: Supervision, Writing – review & editing. Dean C. Webster: Resources, Writing – review & editing. Guodong Du: Conceptualization, Funding acquisition, Supervision, Writing – review & editing.

#### **Declaration of Competing Interest**

The authors declare that they have no known competing financial interests or personal relationships that could have appeared to influence the work reported in this paper.

#### Acknowledgments

This material is based upon work supported in part by the National Science Foundation under Grant No. NSF EPSCoR Award IIA-1355466. R. O. thanks SACM for a scholarship and C. G. thanks the NSF for providing REU support through CHE 1757922.

## Appendix A. Supplementary material

Supplementary data to this article can be found online at https://doi.org/10.1016/j.eurpolymj.2021.110756.

## References

- S. Philip, T. Keshavarz, I. Roy, Polyhydroxyalkanoates: Biodegradable Polymers with a Range of Applications, J. Chem. Technol. Biotechnol. 82 (2007) 233–247.
- [2] A.M. Gumel, M.S.M. Annuar, Y. Chisti, Recent Advances in the Production, Recovery and Applications of Polyhydroxyalkanoates, J. Polym. Environ. 21 (2013) 580–605.
- [3] P. Prasteen, Y. Thushyanthy, T. Mikunthan, M. Prabhaharan, Bio-Plastics an Alternative to Petroleum Based Plastics, Int. J. Res. Stud. Agricultural Sci. 4 (2018) 1–7.
- [4] E.W. Dunn, G.W. Coates, Carbonylative Polymerization of Propylene Oxide: A Multicatalytic Approach to the Synthesis of Poly(3-Hydroxybutyrate), J. Am. Chem. Soc. 132 (2010) 11412–11413.
- [5] Y.-C. Xu, W.-M. Ren, H. Zhou, G.-G. Gu, X.-B. Lu, Functionalized Polyesters with Tunable Degradability Prepared by Controlled Ring-Opening (Co)polymerization of Lactones, Macromolecules 50 (8) (2017) 3131–3142.
- [6] C.M. Thomas, Stereocontrolled ring-opening polymerization of cyclic esters: synthesis of new polyester microstructures, Chem. Soc. Rev. 39 (2010) 165–173.
- [7] Z. Grobelny, S. Golba, J. Jurek-Suliga, Ring-opening polymerization of β-butyrolactone in the presence of alkali metal salts: investigation of initiation course and determination of polymers structure by MALDI-TOF mass spectrometry, Polym. Bull. 76 (10) (2019) 4951–4966.
- [8] M.F. Garcia-Valle, V. Tabernero, T. Cuenca, M.E.G. Mosquera, J. Cano, S. Milione, Biodegradable PHB from rac-β-Butyrolactone: Highly Controlled ROP Mediated by a Pentacoordinated Aluminum Complex, Organometallics 37 (2018) 837–840.
- [9] Z. Zhuo, C. Zhang, Y. Luo, Y. Wang, Y. Yao, D. Yuan, D. Cui, Stereo-selectivity switchable ROP of rac-β-butyrolactone initiated by salan-ligated rare-earth metal

- amide complexes: the key role of the substituents on ligand frameworks, Chem. Commun. 54 (2018) 11998–12001.
- [10] J.M. Longo, M.J. Sanford, G.W. Coates, Ring-Opening Copolymerization of Epoxides and Cyclic Anhydrides with Discrete Metal Complexes: Structure-Property Relationships, Chem. Rev. 116 (2016) 15167–15197.
- [11] R. Yang, G. Xu, C. Lv, B. Dong, L. Zhou, Q. Wang, Zn(HMDS)<sub>2</sub> as a Versatile Transesterification Catalyst for Polyesters Synthesis and Degradation toward a Circular Materials Economy Approach, ACS Sustain. Chem. Eng. 8 (2020) 18347–18353.
- [12] W. Gruszka, L.C. Walker, M.P. Shaver, J.A. Garden, In Situ Versus Isolated Zinc Catalysts in the Selective Synthesis of Homo and Multi-block Polyesters, Macromolecules 53 (2020) 4294–4302.
- [13] J. Bai, X. Xiao, Y. Zhang, J. Chao, X. Chen, β-Pyridylenolate Zinc Catalysts for the Ring-Opening Homo- and Copolymerization of ε-Caprolactone and Lactides, Dalton Trans. 46 (2017) 9846–9858.
- [14] S. Abbina, G. Du, Zinc-catalyzed Highly Isoselective Ring Opening Polymerization of rac-Lactide, ACS Macro. Lett. 3 (2014) 689–692.
- [15] S. Abbina, V.K. Chidara, S. Bian, A. Ugrinov, G. Du, Synthesis of Chiral C<sub>2</sub>-symmetric Bimetallic Zinc Complexes of Amido-Oxazolinates and Their Application in Copolymerization of CO<sub>2</sub> and Cyclohexene Oxide, ChemistrySelect 1 (12) (2016) 3175–3183.
- [16] S. Abbina, V.K. Chidara, G. Du, Ring Opening Copolymerization of Styrene Oxide and Cyclic Anhydrides Using Highly Effective Zinc Amido-Oxazolinate Catalysts, ChemCatChem 9 (2017) 1343–1348.
- [17] M. Shaik, V.K. Chidara, S. Abbina, G. Du, Zinc Amido-Oxazolinate Catalyzed Ring Opening Copolymerization and Terpolymerization of Maleic Anhydride and Epoxides, Molecules 25 (18) (2020) 4044.
- [18] T. Ebrahimi, D.C. Aluthge, S.G. Hatzikiriakos, P. Mehrkhodavandi, Highly Active Chiral Zinc Catalysts for Immortal Polymerization of β-Butyrolactone form Melt Processable Syndio-Rich Poly(hydroxybutyrate), Macromolecules 49 (23) (2016) 8812–8824
- [19] C.G. Jaffredo, J.-F. Carpentier, S.M. Guillaume, Poly(hydroxyalkanoate) Block or Random Copolymers of β-Butyrolactone and Benzyl β-Malolactone: A Matter of Catalytic Tuning, Macromolecules 46 (17) (2013) 6765–6776.
- [20] C. Guillaume, J.-F. Carpentier, S.M. Guillaume, Immortal Ring Opening Polymerization of β-Butyrolactone with Zinc Catalysts: Catalytic Approach to Poly (3-hydroxyalkanoate), Polymer 50 (25) (2009) 5909–5917.
- [21] J.W. Kramer, G.W. Coates, Fluorinated β-lactones and Poly(β-hydroxyalkanoate)s: Synthesis via Epoxide Carbonylation and Ring Opening Polymerization, Tetrahedron 64 (29) (2008) 6973–6978.
- [22] W. Zhang, T. Ji, S. Lyon, M. Mehta, Y. Zheng, X. Deng, A. Liu, A. Shagan, B. Mizrahi, D.S. Kohane, Functionalized Multiarmed Polycaprolactones as Biocompatible Tissue Adhesives, ACS Appl. Mater. Interfaces 12 (2020) 17314–17320.
- [23] Y. Deng, S.J. Liu, B.M. Zhao, P. Wang, Q.L. Fan, W. Huang, L.H. Wang, Synthesis and Characterization of one Star-Shaped Polymer with Charged Iridium Complex as Luminescent Core, J. Lumin. 131 (2011) 2166–2173.
- [24] L. Teng, X. Xu, W. Nie, Y. Zhou, L. Song, P. Chen, Synthesis and Degradability of a Star-Shaped Polylactide Based on L-Lactide and Xylitol, J. Polym. Res. 22 (2015) 83.
- [25] I. Yu, T. Ebrahimi, S.G. Hatzikiriakos, P. Mehrkhodavandi, Star-Shaped PHB–PLA block copolymers: immortal polymerization with dinuclear indium catalysts, Dalton Trans. 44 (2015) 14248–14254.
- [26] B.S. Lele, J.C. Leroux, Synthesis of Novel Amphiphilic Star-Shaped Poly(1-caprolactone)-Block- Poly(N-(2-hydroxypropyl)methacrylamide) by Combination of Ring-Opening and Chain Transfer Polymerization, Polymer 43 (2002) 5595–5606.
- [27] P.T. Dirlam, D.J. Goldfeld, D.C. Dykes, M.A. Hillmyer, Polylactide Foams with Tunable Mechanical Properties and Wettability using a Star Polymer Architecture and a Mixture of Surfactants, ACS Sustain. Chem. Eng. 7 (2019) 1698–1706.
- [28] A. Michalski, M. Brzezinski, G. Lapienis, T. Biela, Star-Shaped and Branched Polylactides: Synthesis, Characterization, and Properties, Prog. Polym. Sci. 89 (2019) 159–212.
- [29] I. Gadwal, P.P. Wadgaonkar, A.B. Ichake, S.R. Mane, A New Approach for the Synthesis of Miktoarm Star Polymers through a Combination of Thiol-Epoxy "Click" Chemistry and ATRP/Ring-Opening Polymerization Techniques, J. Polym. Sci., Part A: Polym. Chem. 57 (2019) 146–156.

- [30] J. Cheng, J.X. Ding, Y.C. Wang, J. Wang, Synthesis and Characterization of Star-Shaped Block Copolymer of Poly(ε-Caprolactone) and Poly(Ethyl Ethylene Phosphate) as Drug Carrier, Polymer 49 (2008) 4784–4790.
- [31] P. Pahl, C. Schwarzenböck, F.A.D. Herz, B.S. Soller, C. Jandl, B. Rieger, Core-First Synthesis of Three-Armed Star-Shaped Polymers by Rare Earth Metal-Mediated Group Transfer Polymerization, Macromolecules 50 (17) (2017) 6569–6576.
- [32] J.M. Ren, T.G. McKenzie, Q. Fu, E.H.H. Wong, J. Xu, Z. An, S. Shanmugam, T. P. Davis, C. Boyer, G.G. Qiao, Star Polymers, Chem. Rev. 116 (2016) 6743–6836.
- [33] T. Ebrahimi, S.G. Hatzikiriakos, P. Mehrkhodavandi, Synthesis and Rheological Characterization of Star Shaped and Linear Poly(hydroxybutyrate), Macromolecules 48 (2015) 6672–6681.
- [34] G. Barouti, S.S. Liow, Q. Dou, H. Ye, C. Orione, S.M. Guillaume, X.J. Loh, New Linear and Star-Shaped Thermogelling Poly([R]-3-hydroxybutyrate) Copolymers, Chem. Eur. J. 22 (2016) 10501–10512.
- [35] M. Shaik, J. Peterson, G. Du, Cyclic and Linear Polyhydroxylbutyrates from Ring-Opening Polymerization of β-Butyrolactone with Amido-Oxazolinate Zinc Catalysts, Macromolecules 52 (1) (2019) 157–166.
- [36] R.A. Sheldon, Green and sustainable manufacture of chemicals from biomass: state of the art Green Chem. 16 (2014) 950–963.
- [37] T. Takei, N. Iguchi, M. Haruta, Synthesis of Acetaldehyde, Acetic Acid, and Others by the Dehydrogenation and Oxidation of Ethanol, Catal. Surv. Asia 15 (2011) 80–88.
- [38] C. J. Kenneally, G. A. Busch, P. J. Corrigan, E. P. Granberg, J. K. Howie, R. G. Schafermeyer, J. E. Trout, Process for synthesis of polyol fatty acid polyesters. US Patent 6121440A, 2000.
- [39] S. Ma, D.C. Webster, F. Jabeen, Hard and Flexible, Degradable Thermosets from Renewable Bioresources with the Assistance of Water and Ethanol, Macromolecules 49 (2016) 3780–3788.
- [40] R.P. Chitemere, S. Stafslien, B. Rasulev, D.C. Webster, M. Quadir, Soysome: A Surfactant-Free, Fully Biobased, Self-Assembled Platform for Nanoscale Drug Delivery Applications, ACS Appl. Bio Mater. 1 (2018) 1830–1841.
- [41] V.K. Chidara, S. Stadem, D.C. Webster, G. Du, Survey of Several Catalytic Systems for the Epoxidation of a Biobased Ester Sucrose Soyate, Catal. Commun. 111 (2018) 31–35.
- [42] P. Binda, S. Abbina, G. Du, Modular Synthesis of Chiral β- Diketiminato-Type Ligands Containing 2-Oxazoline Moiety via Palladium-Catalyzed Amination, Synthesis 2011 (16) (2011) 2609–2618.
- [43] S. Abbina, G. Du, Chiral Amido-Oxazolinate Zinc Complexes for Asymmetric Alternating Copolymerization of CO<sub>2</sub> and Cyclohexene Oxide, Organometallics 31 (21) (2012) 7394–7403.
- [44] Gwyddion software, version 2.55, http://gwyddion.net/.
- [45] N. Fazeli, N. Mohammadi, F.A. Taromi, A Relationship Between Hydrodynamic and Static Properties of Star-Shaped Polymers, Polym. Testing 23 (2004) 431–435.
- [46] W. Zhang, S. Zheng, Synthesis and Characterization of Dendritic Star Poly(L-Lactide)s, Polym. Bull. 58 (2007) 767–775.
- [47] E. Grunova, E. Kirillov, T. Roisnel, J.F. Carpentier, Group 3 metal complexes supported by tridentate pyridine-and thiophene linked bis(naphtholate) ligands: synthesis, structure, and use in stereoselective ring-opening polymerization of racemic lactide and β-butyrolactone, Dalton Trans. 39 (2010) 6739–6752.
- [48] T.J. Nelson, B. Masaki, Z. Morseth, D.C. Webster, Highly Functional Biobased Polyols and Their Use in Melamine-Formaldehyde Coatings, J. Coat. Technol. Res. 10 (2013) 757–767.
- [49] R. Wang, T.P. Schuman, Vegetable Oil-Derived Epoxy Monomers and Polymer Blends A Comparative Study with Review, eXPRESS Polym. Lett. 7 (2013) 272–292.
- [50] A.M. Salih, M.B. Ahmad, N.A. Ibrahim, K.Z.H.M. Dahlan, R. Tajau, M.H. Mahmood, W.M.Z.W. Yunus, Synthesis of Radiation Curable Palm Oil-Based Epoxy Acrylate: NMR and FTIR Spectroscopic Investigations, Molecules 20 (2015) 14191–14211.
- [51] Z. Guo, X. Chen, J. Xin, D. Wu, J. Li, C. Xu, Effect of Molecular Weight and Arm Number on the Growth and pH-Dependent Morphology of Star Poly(2-(dimethylamino)ethyl methacrylate]/Poly(styrenesulfonate) Multilayer Films, Macromolecules 43 (2010) 9087–9093.
- [52] W. Xie, N. Jiang, Z. Gan, Effects of Multi-Arm Structure on Crystallization and Biodegradation of Star-Shaped Poly(e-caprolactone), Macromol. Biosci. 8 (2008) 775–784.
- [53] P.F. Green, V. Ganesan, Dewetting of polymeric films: unresolved issues, Eur. Phys. J. E 12 (3) (2003) 449–454.
- [54] E. Glynos, A. Chremos, B. Frieberg, G. Sakellariou, P.F. Green, Wetting of Macromolecules: From Linear Chain to Soft Colloid-Like Behavior, Macromolecules 47 (3) (2014) 1137–1143.